# Low-Complexity Equalization of MIMO-OSDM

Han, Jing; Ma, Shengqian; Wang, Yujie; Leus, Geert

**DOI**
10.1109/TVT.2019.2957542

**Publication date**
2020

**Document Version**
Final published version

**Published in**
IEEE Transactions on Vehicular Technology

# Low-Complexity Equalization of MIMO-OSDM

Jing Han, *Member, IEEE*, Shengqian Ma, Yujie Wang, and Geert Leus, *Fellow, IEEE*

***Abstract*—Orthogonal signal-division multiplexing (OSDM) is an attractive alternative to conventional orthogonal frequency-division multiplexing (OFDM) due to its enhanced ability in peak-to-average power ratio (PAPR) reduction. Combining OSDM with multiple-input multiple-output (MIMO) signaling has the potential to achieve high spectral and power efficiency. However, a direct channel equalization in this case incurs a cubic complexity, which may be expensive for practical use. To solve the problem, low-complexity per-vector and block equalization algorithms of MIMO-OSDM are proposed in this paper for time-invariant and time-varying channels, respectively. By exploiting the channel matrix structures, these algorithms have only a linear complexity in the transformed domain. Simulation results demonstrate their validity and the related performance comparisons.**

***Index Terms*—MIMO, OSDM, inter-vector interference, equalization, underwater acoustic communication.**

## I. Introduction

Multiple-input multiple-output (MIMO) signaling is a powerful technique to enhance the system spectral efficiency and/or to achieve spatial diversity gain [1]. For years there has been a lasting interest on its combination with orthogonal frequency-division multiplexing (OFDM). One of the main reasons for this is that OFDM is capable of converting a time-invariant (TI) frequency-selective channel into a parallel set of frequency-flat channels, thus enabling simple equalization to mitigate inter-symbol interference (ISI). In addition, over time-varying (TV) channels, although inter-carrier interference (ICI) arises in this case due to the loss of orthogonality among subcarriers, low-complexity MIMO equalization is still feasible by restricting ICI support [2], [3]. However, it is well known that the high peak-to-average power ratio (PAPR) of OFDM may lead to a substantial penalty in the power efficiency of MIMO systems [4].

In contrast, single-carrier block transmission (SCBT) has a lower PAPR and thus a better power efficiency. By combining it with continuous phase modulation, an improved spectral efficiency can also be achieved [5], [6]. Furthermore, at the receiver single-carrier frequency-domain equalization [7] and other reduced-complexity signal detection techniques [8] can be applied to combat TI or TV channel fading. As such, SCBT is a popular alternative to OFDM in some MIMO scenarios [9]. However, these good properties come at the cost of the flexibility in the management of bandwidth resources, i.e., SCBT cannot perform bit loading as OFDM.

As a new modulation scheme, orthogonal signal-division multiplexing (OSDM) has a similar signal structure as vector OFDM in [10], and provides a generalized framework incorporating OFDM and SCBT as two extremes [11], [12]. Specifically, unlike conventional OFDM, where the data block is treated as a whole and modulated by a single full-length inverse discrete Fourier transform (IDFT), OSDM splits the data block into segments, termed vectors, and performs several component-wise IDFTs among them. By adjusting the vector length, OSDM can achieve flexible tradeoffs between the PAPR and the bandwidth management ability [12].

Thanks to this appealing feature, OSDM has recently received much attention, especially in underwater acoustic (UWA) communications [12]–[15]. However, so far most efforts have been focused on the single-transmitter case, and there exist very limited studies on MIMO-OSDM. Among them, in [16] Alamouti-like space-time and space-frequency block coding systems were investigated over TI channels, while in [17] a spatial multiplexing scheme was designed for TV channels. The latter is particularly useful for high-rate UWA communications, where the channel bandwidth is extremely narrow and the influence of the PAPR is more pronounced. However, the equalizer in [17] performs direct channel matrix inversion, which leads to a cubic complexity.

The motivation of this paper is to implement channel equalization of MIMO-OSDM with a similar complexity as its OFDM counterpart. To this end, low-complexity per-vector and block equalization algorithms are proposed for TI and TV channels, respectively. Our contributions are as follows.

- OSDM has different interference structures compared to OFDM. Over TI channels, while OFDM symbols on each subcarrier can be decoupled, OSDM suffers from intra-vector ISI. Also, over TV channels, analogous to ICI in OFDM, inter-vector interference (IVI) arises in OSDM. To mitigate these effects efficiently, instead of being performed directly in the frequency domain as OFDM equalization, the proposed MIMO-OSDM equalization algorithms are implemented in a transformed domain.
- The equalizers proposed in this paper are an extension of the single-input single-output (SISO) algorithms in [11], [15]. However, other than a simple increase in dimensionality, a special pre-processing of interleaving is further performed. Such operation can produce a block-diagonal channel matrix structure for the TI case, and achieve a block-banded channel matrix approximation for the TV case based on the complex exponential basis expansion model (CE-BEM). These matrix structures enable a linear complexity of the proposed equalization algorithms in the transformed domain.

*Notation:* $(\cdot)^*$ stands for conjugate, $(\cdot)^T$ for transpose, and $(\cdot)^H$ for Hermitian transpose. We define $[\mathbf{x}]_{m:n}$ as the subvector of $\mathbf{x}$ from entry $m$ to $n$, and $[\mathbf{X}]_{m:n,p:q}$ as the submatrix of $\mathbf{X}$ from row $m$ to $n$ and from column $p$ to $q$, where all indices are starting from 0. Moreover, $\mathrm{diag}\{\mathbf{x}\}$ represents a diagonal matrix with $\mathbf{x}$ on its diagonal, and $\mathrm{Diag}\{\mathbf{A}_0,\ldots,\mathbf{A}_{N-1}\}$ represents a block-diagonal matrix created with the submatrices $\{\mathbf{A}_n\}_{n=0}^{N-1}$. Also, $\mathbf{F}_N$ stands for the $N\times N$ unitary discrete Fourier transform (DFT) matrix; $\mathbf{I}_N$ and $\mathbf{e}_N(n)$ refer to the $N\times N$ identity matrix and its $n$th column, respectively; $\mathbf{0}_N$ denotes the $N\times 1$ all-zero vector; $\mathbf{P}_{M,N}$ is the $MN\times MN$ permutation matrix

Manuscript received June 26, 2019; revised October 24, 2019; accepted December 1, 2019. Date of publication December 4, 2019; date of current version February 12, 2020. This work was supported in part by the National Natural Science Foundation of China under Grants 61771394, 61531015, and 61801394; in part by the Natural Science Basic Research Plan in Shaanxi Province of China under Grant 2018JM6042; and in part by 111 Project under Grant B18041. The review of this article was coordinated by Prof. S.-H. Leung. *(Corresponding author: Jing Han.)*

J. Han, S. Ma, and Y. Wang are with the School of Marine Science and Technology, Northwestern Polytechnical University, Xi'an 710072, China (e-mail: hanj@nwpu.edu.cn; sqma@mail.nwpu.edu.cn; yjwang@mail.nwpu.edu.cn).

G. Leus is with the Faculty of Electrical Engineering, Mathematics and Computer Science, Delft University of Technology, Delft 2826 CD, The Netherlands (e-mail: g.j.t.leus@tudelft.nl).

Digital Object Identifier 10.1109/TVT.2019.2957542

defined as

$$\mathbf{P}_{M,N} = \begin{bmatrix} \mathbf{I}_M \otimes \mathbf{e}_N^T(0) \\ \mathbf{I}_M \otimes \mathbf{e}_N^T(1) \\ \vdots \\ \mathbf{I}_M \otimes \mathbf{e}_N^T(N-1) \end{bmatrix},$$

where $\otimes$ denotes the Kronecker product.

## II. Equalization Over TI Channels

Consider a MIMO-OSDM system with $U$ transmitters and $V$ receivers. The symbol block at the $u$th transmitter, denoted by $\mathbf{d}^{(u)}$, is from a PSK or QAM constellation and of length $K = MN$. Unlike OFDM modulation which uses a single length-$K$ IDFT, OSDM modulation can be expressed as

$$\mathbf{s}^{(u)} = \left(\mathbf{F}_N^H \otimes \mathbf{I}_M\right) \mathbf{d}^{(u)}, \tag{1}$$

for $u = 1, 2, \ldots, U$. A PAPR reduction is achieved, since it contains $M$ (shorter) IDFTs among $N$ symbol vectors

$$\mathbf{d}_n^{(u)} = [\mathbf{d}^{(u)}]_{nM:nM+M-1}, \tag{2}$$

for $n = 0, 1, \ldots, N-1$. Then, after a cyclic prefix (CP) insertion, the block is transmitted through channels.

Let us first assume that all the channels are time invariant and denote the channel impulse response (CIR) between the $u$th transmitter and the $v$th receiver by $\mathbf{c}^{(v,u)} = [c_0^{(v,u)}, c_1^{(v,u)}, \ldots, c_L^{(v,u)}]^T$, where $L$ is the channel order. In this case, the received signal block at the $v$th receiver after CP removal has the form

$$\mathbf{r}^{(v)} = \sum_{u=1}^{U} \tilde{\mathbf{C}}^{(v,u)} \mathbf{s}^{(u)} + \mathbf{w}^{(v)}, \tag{3}$$

for $v = 1, 2, \ldots, V$, where $\tilde{\mathbf{C}}^{(v,u)}$ is the $K \times K$ circulant channel matrix with its first column being $[\mathbf{c}^{(v,u)T}, \mathbf{0}_{K-L-1}^T]^T$; $\mathbf{w}^{(v)}$ is the $K \times 1$ received noise.

Subsequently, OSDM demodulation is performed as

$$\mathbf{x}^{(v)} = \left(\mathbf{F}_N \otimes \mathbf{I}_M\right) \mathbf{r}^{(v)} = \sum_{u=1}^{U} \mathbf{C}^{(v,u)} \mathbf{d}^{(u)} + \mathbf{z}^{(v)}, \tag{4}$$

where $\mathbf{C}^{(v,u)} = (\mathbf{F}_N \otimes \mathbf{I}_M)\tilde{\mathbf{C}}^{(v,u)}(\mathbf{F}_N^H \otimes \mathbf{I}_M)$ is termed the composite channel matrix; $\mathbf{z}^{(v)}$ is the $K \times 1$ demodulated noise. It can be easily verified from (1) and (4) that, when $M = 1$ ($N = K$) and $M = K$ ($N = 1$), the signal model of MIMO-OSDM is equivalent to that of MIMO-OFDM and MIMO-SCBT, respectively. In this sense, MIMO-OSDM can be deemed as a more generalized MIMO scheme.

Moreover, for TI channels, it is known that the composite channel matrix has the block-diagonal structure [12], [15]

$$\mathbf{C}^{(v,u)} = \mathrm{Diag}\left\{\mathbf{H}_0^{(v,u)}, \mathbf{H}_1^{(v,u)}, \ldots, \mathbf{H}_{N-1}^{(v,u)}\right\}, \tag{5}$$

where

$$\mathbf{H}_n^{(v,u)} = \mathbf{\Lambda}_M^{nH} \mathbf{F}_M^H \overline{\mathbf{H}}_n^{(v,u)} \mathbf{F}_M \mathbf{\Lambda}_M^n, \tag{6}$$

$$\overline{\mathbf{H}}_n^{(v,u)} = \mathrm{diag}\left\{H_n^{(v,u)}, H_{n+N}^{(v,u)}, \ldots, H_{n+(M-1)N}^{(v,u)}\right\}, \tag{7}$$

$\mathbf{\Lambda}_M^n = \mathrm{diag}\{[1, e^{-j\frac{2\pi n}{K}}, \ldots, e^{-j\frac{2\pi n}{K}(M-1)}]^T\}$ and $H_k^{(v,u)} = \sum_{l=0}^{L} c_l^{(v,u)} e^{-j\frac{2\pi}{K}lk}$. Given this matrix structure, we partition $\mathbf{x}^{(v)}$ and $\mathbf{z}^{(v)}$ into $N$ vectors of length $M$ as in (2). Since only intra-vector ISI exists in this case, the channel equalization can be decoupled on each vector. Specifically, by defining $\mathbf{x}_n^{(v)} = [\mathbf{x}^{(v)}]_{nM:nM+M-1}$ and $\mathbf{z}_n^{(v)} = [\mathbf{z}^{(v)}]_{nM:nM+M-1}$ for $n = 0, 1, \ldots, N-1$ as the $n$th demodulated vector and noise vector, respectively, it can be readily obtained that

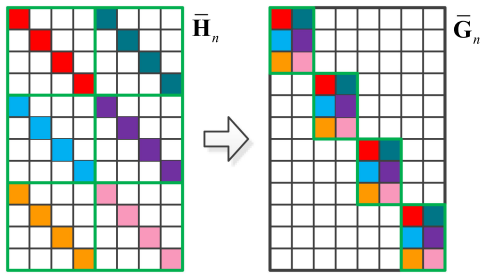


Fig. 1. An example of the TI channel matrix structures of $\overline{\mathbf{H}}_n$ and $\overline{\mathbf{G}}_n$ with $U = 2$, $V = 3$ and $M = 4$.

$$\mathbf{x}_n = \mathbf{H}_n \mathbf{d}_n + \mathbf{z}_n, \tag{8}$$

where we have stacked all the $n$th vectors, i.e., $\mathbf{d}_n = [\mathbf{d}_n^{(1)T}, \mathbf{d}_n^{(2)T}, \ldots, \mathbf{d}_n^{(U)T}]^T$, $\mathbf{x}_n = [\mathbf{x}_n^{(1)T}, \mathbf{x}_n^{(2)T}, \ldots, \mathbf{x}_n^{(V)T}]^T$, $\mathbf{z}_n = [\mathbf{z}_n^{(1)T}, \mathbf{z}_n^{(2)T}, \ldots, \mathbf{z}_n^{(V)T}]^T$, and

$$\mathbf{H}_n = \begin{bmatrix} \mathbf{H}_n^{(1,1)} & \mathbf{H}_n^{(1,2)} & \ldots & \mathbf{H}_n^{(1,U)} \\ \mathbf{H}_n^{(2,1)} & \mathbf{H}_n^{(2,2)} & \ldots & \mathbf{H}_n^{(2,U)} \\ \vdots & \vdots & \ddots & \vdots \\ \mathbf{H}_n^{(V,1)} & \mathbf{H}_n^{(V,2)} & \ldots & \mathbf{H}_n^{(V,U)} \end{bmatrix}. \tag{9}$$

Throughout this paper, we assume that the input symbols on all transmitters are independent and identically distributed (i.i.d.) with unit power, while the noise samples on different receivers are zero mean with the same variance $\sigma^2$. Therefore, based on (8), the minimum mean-square error (MMSE) equalization algorithm can be written as

$$\hat{\mathbf{d}}_n = \left(\mathbf{R}_n^{-1} \mathbf{H}_n^H\right) \mathbf{x}_n. \tag{10}$$

where $\mathbf{R}_n = \mathbf{H}_n^H \mathbf{H}_n + \sigma^2 \mathbf{I}_{UM}$ is an $UM \times UM$ matrix. Since a straightforward computation of $\mathbf{R}_n^{-1}$ will incur a complexity of $\mathcal{O}(U^3 M^3)$, to ease the computational burden, we substitute (6) into (9), yielding

$$\mathbf{H}_n = \mathbf{\Phi}_{n,V}^H \overline{\mathbf{H}}_n \mathbf{\Phi}_{n,U}, \tag{11}$$

where $\mathbf{\Phi}_{n,i} = \mathbf{I}_i \otimes (\mathbf{F}_M \mathbf{\Lambda}_M^n)$; $\overline{\mathbf{H}}_n$ has a similar structure as $\mathbf{H}_n$ in (9) with its blocks replaced by the diagonal matrices $\{\overline{\mathbf{H}}_n^{(v,u)}\}$. Furthermore, as illustrated in Fig. 1, $\overline{\mathbf{H}}_n$ can actually be interleaved into a block-diagonal matrix, i.e.,

$$\begin{aligned} \overline{\mathbf{G}}_n &= \mathbf{P}_{V,M} \overline{\mathbf{H}}_n \mathbf{P}_{U,M}^H \\ &= \mathrm{Diag}\left\{\overline{\mathbf{G}}_{n,0}, \overline{\mathbf{G}}_{n,1}, \ldots, \overline{\mathbf{G}}_{n,M-1}\right\}, \end{aligned} \tag{12}$$

with $\overline{\mathbf{G}}_{n,m}$ being blocks of size $V \times U$.

Based on the matrix factorizations in (11) and (12), the symbol estimation in (10) can be rewritten as

$$\hat{\mathbf{d}}_n = \mathbf{\Phi}_{n,U}^H \mathbf{P}_{U,M}^H \left(\overline{\mathbf{R}}_n^{-1} \overline{\mathbf{G}}_n^H\right) \mathbf{P}_{V,M} \mathbf{\Phi}_{n,V} \mathbf{x}_n, \tag{13}$$

where $\overline{\mathbf{R}}_n = \overline{\mathbf{G}}_n^H \overline{\mathbf{G}}_n + \sigma^2 \mathbf{I}_{UM}$. As shown in Fig. 2(a), (13) actually corresponds to a low-complexity implementation of MIMO-OSDM equalization over TI channels, which consists of five steps:

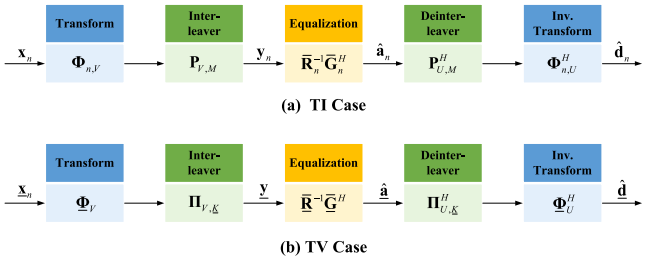


Fig. 2. Proposed TI and TV channel equalization schemes for MIMO-OSDM.

1) Transform the demodulated vector $\mathbf{x}_n$ by $\mathbf{\Phi}_{n,V}$.
2) Interleave the transformed vector by $\mathbf{P}_{V,M}$.
3) Equalize the interleaved vector (denoted by $\mathbf{y}_n$) to obtain the transformed symbol estimate (denoted by $\hat{\mathbf{a}}_n$), i.e.,

$$\hat{\mathbf{a}}_n = \left(\overline{\mathbf{R}}_n^{-1}\overline{\mathbf{G}}_n^H\right)\mathbf{y}_n. \tag{14}$$

4) Deinterleave the output of the equalizer by $\mathbf{P}_{U,M}^H$.
5) Perform the inverse transform $\mathbf{\Phi}_{n,U}^H$ to finally obtain $\hat{\mathbf{d}}_n$.

In this implementation, Steps 1 and 5 involve $V$ DFTs and $U$ IDFTs of length $M$, respectively, resulting in a complexity of $\mathcal{O}((U+V)M\log_2 M)$. As for Step 3, the transformed-domain equalization in (14) may look similar to that in (10); however, its computation is more tractable. To be specific, it can be seen that $\overline{\mathbf{R}}_n$ is a block-diagonal matrix with $M$ blocks of size $U \times U$ on its diagonal, so the inversion in (14) has only a complexity of $\mathcal{O}(U^3M)$, which is linear in the vector length $M$. Given the fact that the values of $U$ and $V$ are typically not large, the total complexity of (13) will be easy to handle.

## III. Equalization Over TV Channels

We proceed to consider the equalization of MIMO-OSDM over TV channels. The CIR between the $u$th transmitter and the $v$th receiver is now denoted by $\{c_{k,l}^{(v,u)}\}$, where the index $k$ is added to embody the time dependence of the CIR. And in this case $\{\mathbf{C}^{(v,u)}\}$ no longer have the block-diagonal structure as in (5); instead, they are generally full matrices. As a result, IVI arises in OSDM, which is a counterpart of ICI in OFDM.

For simplicity, the CE-BEM in [14], [15], [17] is adopted to approximate the TV CIR. It utilizes complex exponential bases to capture the channel time variations in each block, i.e.,

$$c_{k,l}^{(v,u)} = \sum_{q=-Q}^{Q} h_{q,l}^{(v,u)} e^{j\frac{2\pi}{K}qk}, \tag{15}$$

for $k = 0, 1, \ldots, K-1$, where $Q$ is the discrete Doppler spread and $\{h_{q,l}^{(v,u)}\}$ are the BEM coefficients. With this model, the number of channel parameters on each delay tap $l$ is reduced from $K$ to $2Q+1$. Moreover, based on (15), we have the TV channel matrix

$$\tilde{\mathbf{C}}^{(v,u)} = \sum_{q=-Q}^{Q} \tilde{\mathbf{\Gamma}}_K^q \tilde{\mathbf{C}}_q^{(v,u)}, \tag{16}$$

where $\tilde{\mathbf{\Gamma}}_K^q = \text{diag}\{[1, e^{j\frac{2\pi}{K}q}, \ldots, e^{j\frac{2\pi}{K}q(K-1)}]^T\}$; $\tilde{\mathbf{C}}_q^{(v,u)}$ is a circulant matrix with its first column equal to $\mathbf{h}_q^{(v,u)} = [h_{q,0}^{(v,u)}, h_{q,1}^{(v,u)}, \ldots, h_{q,L}^{(v,u)}]^T$ appended by $K-L-1$ zeros. Note that, as shown in the left of Fig. 3, the composite channel matrix $\mathbf{C}^{(v,u)}$ corresponding to (16) is (cyclically) block-banded with block semi-bandwidth (BSB) $Q$ (see [15, Proposition 3] for a proof), which lays the foundation for our low-complexity equalization algorithm in this section.

Specifically, the presence of IVI excludes the use of the per-vector equalization algorithm previously designed for TI channels. We thus consider a block equalization for TV channels, which jointly estimates all symbol vectors in an OSDM block. Moreover, to achieve a low-complexity implementation, we again resort to matrix factorization of the blocks in $\mathbf{C}^{(v,u)}$. Let $\mathbf{C}_{n,n'}^{(v,u)} = [\mathbf{C}^{(v,u)}]_{nM:nM+M-1,n'M:n'M+M-1}$ be the $(n,n')$th block of $\mathbf{C}^{(v,u)}$. It has been shown in [15, Proposition 4] that only blocks in the main band of $\mathbf{C}^{(v,u)}$ can be diagonalized. More specifically, only when $|n-n'| \le Q$, we have

$$\mathbf{C}_{n,n'}^{(v,u)} = \mathbf{\Lambda}_M^{nH}\mathbf{F}_M^H\overline{\mathbf{H}}_{n-n',n'}^{(v,u)}\mathbf{F}_M\mathbf{\Lambda}_M^{n'}, \tag{17}$$

where

$$\overline{\mathbf{H}}_{q,n}^{(v,u)} = \text{diag}\{[H_{q,n}^{(v,u)}, H_{q,N+n}^{(v,u)}, \ldots, H_{q,(M-1)N+n}^{(v,u)}]^T\}, \tag{18}$$

and $H_{q,k}^{(v,u)} = \sum_{l=0}^{L} h_{q,l}^{(v,u)} e^{-j\frac{2\pi}{K}lk}$ for $k = 0, 1, \ldots K-1$.

To eliminate the blocks in the bottom-left and top-right corners of $\mathbf{C}^{(v,u)}$ (which cannot be diagonalized), at each transmitter we place $Q$ zero vectors at both edges of the symbol block, i.e., $\mathbf{d}^{(u)} = [\mathbf{0}_{MQ}^T, \underline{\mathbf{d}}^{(u)T}, \mathbf{0}_{MQ}^T]^T$, where $\underline{\mathbf{d}}^{(u)} = \mathbf{T}\mathbf{d}^{(u)}$ contains the middle $\underline{N} = N - 2Q$ payload vectors with $\mathbf{T} = [\mathbf{I}_K]_{QM:(N-Q)M-1,1:K}$. Accordingly, at each receiver the demodulated block is truncated as $\underline{\mathbf{x}}^{(v)} = \mathbf{T}\mathbf{x}^{(v)}$. Then, it can be obtained that

$$\underline{\mathbf{x}}^{(v)} = \sum_{u=1}^{U} \underline{\mathbf{C}}^{(v,u)}\underline{\mathbf{d}}^{(u)} + \underline{\mathbf{z}}^{(v)}, \tag{19}$$

where $\underline{\mathbf{C}}^{(v,u)} = \mathbf{T}\mathbf{C}^{(v,u)}\mathbf{T}^H$ and $\underline{\mathbf{z}}^{(v)}$ is the noise term. As shown in Fig. 3, $\underline{\mathbf{C}}^{(v,u)}$ is a standard (not cyclically) block-banded matrix. Based on (17), it can be further factorized into

$$\underline{\mathbf{C}}^{(v,u)} = \underline{\mathbf{\Omega}}^H\overline{\underline{\mathbf{C}}}^{(v,u)}\underline{\mathbf{\Omega}}, \tag{20}$$

where $\underline{\mathbf{\Omega}} = \text{Diag}\{\mathbf{F}_M\mathbf{\Lambda}_M^Q, \mathbf{F}_M\mathbf{\Lambda}_M^{Q+1}, \ldots, \mathbf{F}_M\mathbf{\Lambda}_M^{N-Q-1}\}$; $\overline{\underline{\mathbf{C}}}^{(v,u)}$ has the same matrix structure as $\underline{\mathbf{C}}^{(v,u)}$, but with all its nonzero blocks being diagonal (see Fig. 3).

Now, let us stack all these blocks of length $\underline{K} = M\underline{N}$, and define $\underline{\mathbf{d}} = [\underline{\mathbf{d}}^{(1)T}, \underline{\mathbf{d}}^{(2)T}, \ldots, \underline{\mathbf{d}}^{(U)T}]^T$, $\underline{\mathbf{x}} = [\underline{\mathbf{x}}^{(1)T}, \underline{\mathbf{x}}^{(2)T}, \ldots, \underline{\mathbf{x}}^{(V)T}]^T$, $\underline{\mathbf{z}} = [\underline{\mathbf{z}}^{(1)T}, \underline{\mathbf{z}}^{(2)T}, \ldots, \underline{\mathbf{z}}^{(V)T}]^T$. From (19) and (20), we then have the signal model

$$\underline{\mathbf{x}} = \underline{\mathbf{C}}\underline{\mathbf{d}} + \underline{\mathbf{z}}, \tag{21}$$

where $\underline{\mathbf{C}} = \underline{\mathbf{\Phi}}_V^H\overline{\underline{\mathbf{C}}}\underline{\mathbf{\Phi}}_U$, with $\underline{\mathbf{\Phi}}_i = \mathbf{I}_i \otimes \underline{\mathbf{\Omega}}$ and

$$\overline{\underline{\mathbf{C}}} = \begin{bmatrix} \overline{\underline{\mathbf{C}}}^{(1,1)} & \overline{\underline{\mathbf{C}}}^{(1,2)} & \cdots & \overline{\underline{\mathbf{C}}}^{(1,U)} \\ \overline{\underline{\mathbf{C}}}^{(2,1)} & \overline{\underline{\mathbf{C}}}^{(2,2)} & \cdots & \overline{\underline{\mathbf{C}}}^{(2,U)} \\ \vdots & \vdots & \ddots & \vdots \\ \overline{\underline{\mathbf{C}}}^{(V,1)} & \overline{\underline{\mathbf{C}}}^{(V,2)} & \cdots & \overline{\underline{\mathbf{C}}}^{(V,U)} \end{bmatrix}. \tag{22}$$

As illustrated in the right of Fig. 3, the matrix structure of $\overline{\underline{\mathbf{C}}}$ can be further simplified by interleaving, i.e.,

$$\overline{\underline{\mathbf{G}}} = \mathbf{P}_{V,\underline{K}}\overline{\underline{\mathbf{B}}}\mathbf{P}_{U,\underline{K}}^H = \mathbf{\Pi}_{V,\underline{K}}\overline{\underline{\mathbf{C}}}\mathbf{\Pi}_{U,\underline{K}}^H, \tag{23}$$

where $\mathbf{\Pi}_{i,\underline{K}} = \mathbf{P}_{i,\underline{K}}(\mathbf{I}_i \otimes \mathbf{P}_{\underline{N},M})$, and the resulting matrix $\overline{\underline{\mathbf{G}}}$ is block-banded with block size $V \times U$ and BSB $Q$.

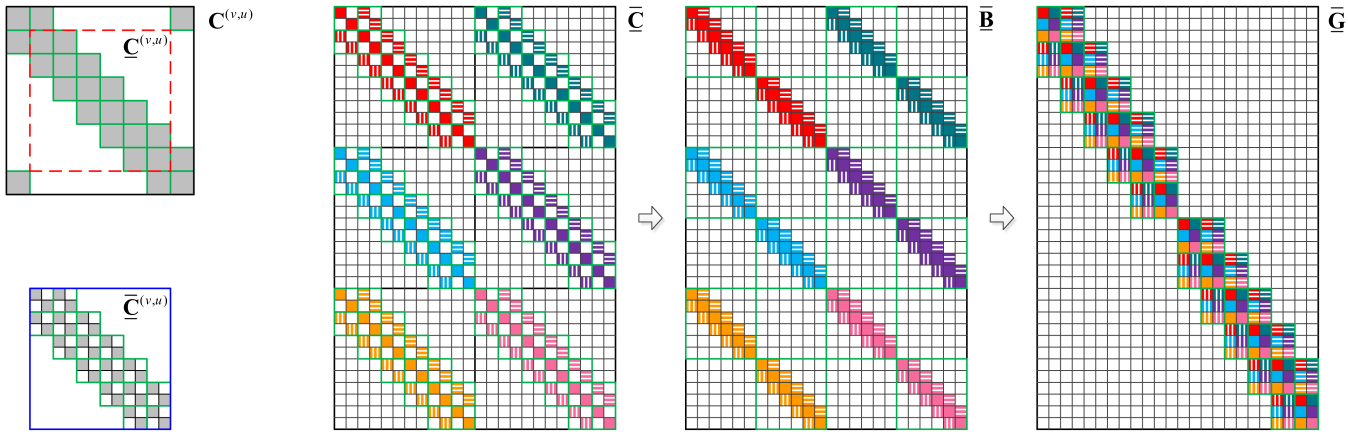


Fig. 3. An example of the TV channel matrix structures with $U = 2$, $V = 3$, $M = 2$, $N = 8$ and $Q = 1$.

Therefore, the MMSE equalization of MIMO-OSDM over TV channels can be written as

$$\hat{\underline{\mathbf{d}}} = \left(\underline{\mathbf{R}}^{-1}\underline{\mathbf{C}}^{H}\right)\underline{\mathbf{x}} \tag{24}$$

$$= \underline{\mathbf{\Phi}}_{U}^{H}\underline{\mathbf{\Pi}}_{U,\underline{K}}^{H}\left(\overline{\underline{\mathbf{R}}}^{-1}\overline{\underline{\mathbf{G}}}^{H}\right)\underline{\mathbf{\Pi}}_{V,\underline{K}}\underline{\mathbf{\Phi}}_{V}\underline{\mathbf{x}}, \tag{25}$$

where $\underline{\mathbf{R}} = \underline{\mathbf{C}}^{H}\underline{\mathbf{C}} + \sigma^2\mathbf{I}_{U\underline{K}}$ and $\overline{\underline{\mathbf{R}}} = \overline{\underline{\mathbf{G}}}^{H}\overline{\underline{\mathbf{G}}} + \sigma^2\mathbf{I}_{U\underline{K}}$. The above equations (24) and (25) represent the direct and low-complexity implementations, respectively. While (24) suffers from a cubic complexity of $\mathcal{O}\{U^3\underline{K}^3\}$, as shown in Fig. 2(b), (25) actually takes the same strategy as (13) to reduce the computational burden. Specifically, here $\underline{\mathbf{x}}$ is first transformed and interleaved into $\underline{\mathbf{y}} = \underline{\mathbf{\Pi}}_{V,\underline{K}}\underline{\mathbf{\Phi}}_{V}\underline{\mathbf{x}}$, on which the TV channel equalization is then performed as

$$\hat{\underline{\mathbf{a}}} = (\overline{\underline{\mathbf{R}}}^{-1}\overline{\underline{\mathbf{G}}}^{H})\underline{\mathbf{y}}, \tag{26}$$

and finally the estimate of the symbol blocks is produced by $\hat{\underline{\mathbf{d}}} = \underline{\mathbf{\Phi}}_{U}^{H}\underline{\mathbf{\Pi}}_{U,\underline{K}}^{H}\hat{\underline{\mathbf{a}}}$. It is easy to see that $\overline{\underline{\mathbf{R}}}$ is a block-banded matrix with block size $U \times U$ and BSB $2Q$. As a result, we can use the block LDL$^H$ algorithm in [15] to compute the matrix inversion in (26), and the complexity is only $\mathcal{O}\{U^3Q^2\underline{K}\}$.

## IV. Numerical Results

In this section, the bit-error rate (BER) performances of the proposed equalization algorithms are evaluated by numerical simulations. We here consider a MIMO-OSDM system in a UWA communication scenario. At each transmitter, OSDM blocks are composed of $K = 1024$ QPSK symbols with symbol period $T_{\mathrm{s}} = 0.25$ ms, and thus the block duration is $T = KT_{\mathrm{s}} = 256$ ms. The MIMO channel is assumed to have an order of $L = 24$, corresponding to a multipath delay spread of $\tau_{\max} = LT_{\mathrm{s}} = 6$ ms, with all the taps Rayleigh distributed and generated from a uniform power delay profile. We first focus on TI channel equalization in Fig. 4, where $2 \times 3$ and $2 \times 4$ systems are investigated against various settings of the vector length, $M = 1$ (i.e., MIMO-OFDM), 4 and 16. Also, the performance of SISO transmission (i.e., $1 \times 1$) based on the equalization algorithm in [11] is included for comparison. As expected, a lower BER is achieved with a larger $V$ thanks to the enhanced spatial diversity. In addition, it is shown that, with $U$ and $V$ fixed, the BER still improves as the vector length gets longer. This can be attributed to the intra-vector frequency diversity inherent in OSDM systems [11], [12].

Figs. 5 and 6 further present the performance of TV channel equalization, where the channel time variation is simulated by a U-shaped

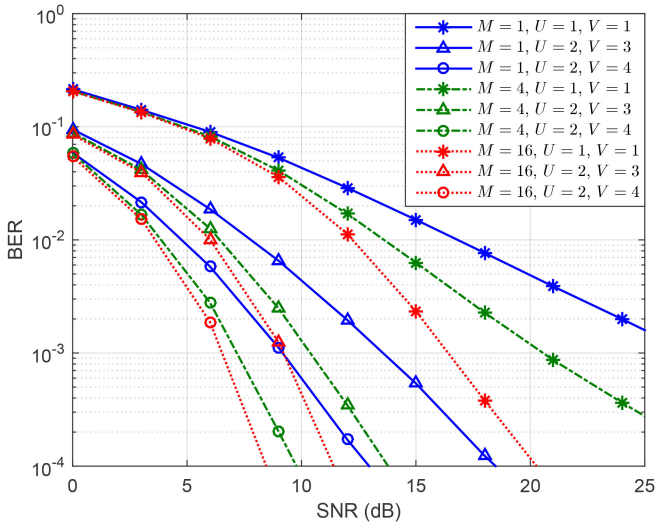


Fig. 4. BER performance of MIMO-OSDM equalization over TI channels for various $M$, $U$ and $V$.

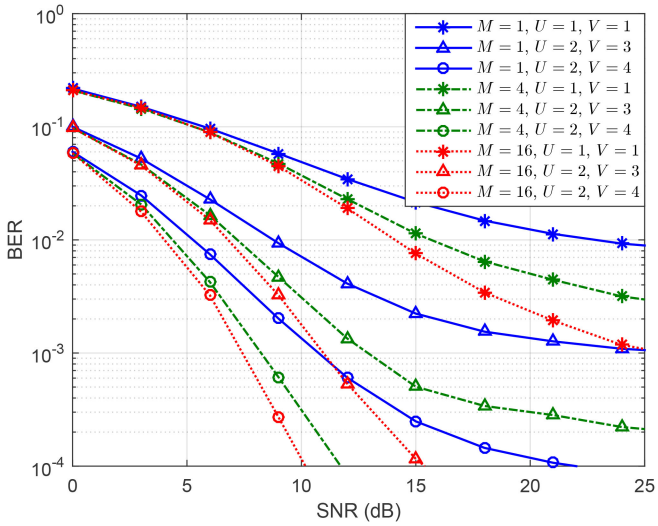


Fig. 5. BER performance of MIMO-OSDM equalization over TV channels for various $M$, $U$ and $V$, given $f_dT = 0.25$ and $Q = 2$.

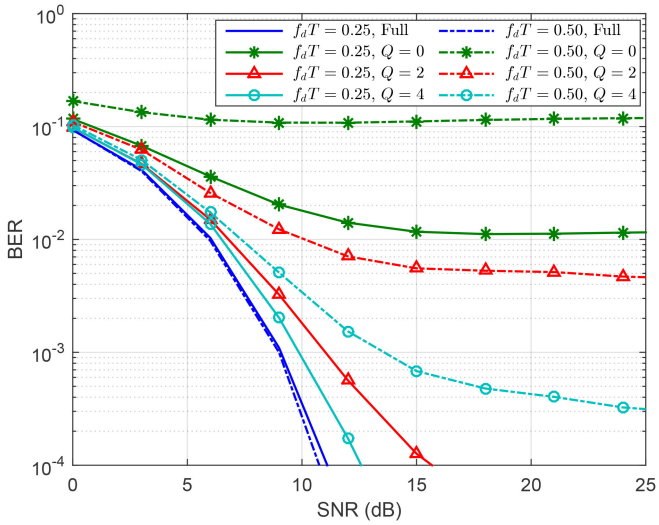


Fig. 6. BER performance of MIMO-OSDM equalization over TV channels for various $f_dT$ and $Q$, given $M = 16$, $U = 2$ and $V = 3$.

Doppler spectrum. Specifically, in Fig. 5, we set the normalized Doppler spread to $f_dT = 0.25$ and the CE-BEM parameter to $Q = 2$. The SISO performance in this case corresponds to the equalization algorithm in [15]. It can be seen that, unlike the TI case in Fig. 4, a BER floor is here induced by the channel approximation error of the CE-BEM. Alternatively, in Fig. 6, we fix $U = 2, V = 3$ and $M = 16$, and compare its performance with that of the direct equalization algorithm in (24), which uses the full channel matrix. A similar observation is made that the block-banded channel matrix approximation based on the CE-BEM leads to a BER gap. However, it is also indicated that the performance loss can be much alleviated by increasing $Q$. More importantly, the proposed MIMO-OSDM equalizer achieves a significant reduction in complexity. As an example, when $M = 16$ and $Q = 4$, the complexity of the proposed algorithm is only $0.008\%$ of that of the direct equalization.

## V. Conclusion

Low-complexity equalization algorithms of MIMO-OSDM are proposed in this paper for TI and TV channels. Compared to the direct equalization method of cubic complexity, they have only a linear complexity in the transformed domain and thus are promising for practical use.

## References

[1] A. J. Paulraj, D. A. Gore, R. U. Nabar, and H. Bolcskei, "An overview of MIMO communications—A key to gigabit wireless," *Proc. IEEE*, vol. 92, no. 2, pp. 198–218, Feb. 2004.
[2] J. Kim, R. W. Heath, and E. J. Powers, "Receiver designs for Alamouti coded OFDM systems in fast fading channels," *IEEE Trans. Wireless Commun.*, vol. 4, no. 2, pp. 550–559, Mar. 2005.
[3] L. Rugini and P. Banelli, "Banded equalizers for MIMO-OFDM in fast time-varying channels," in *Proc. Eur. Signal Process. Conf.*, Sep. 2006, pp. 1–5.
[4] Y. Rahmatallah and S. Mohan, "Peak-to-average power ratio reduction in OFDM systems: A survey and taxonomy," *IEEE Commun. Surv. Tut.*, vol. 15, no. 4, pp. 1567–1592, Oct. 2013.
[5] R. Chayot, N. Thomas, C. Poulliat, M. Boucheret, G. Lesthievent, and N. Van Wambeke, "A frequency-domain band-MMSE equalizer for continuous phase modulation over frequency-selective time-varying channels," in *Proc. Eur. Signal Process. Conf.*, Sep. 2018, pp. 1287–1291.
[6] R. Chayot, N. Thomas, C. Poulliat, M. Bouchcret, N. Van Wambeke, and G. Lesthievent, "Doubly-selective channel estimation for continuous phase modulation," in *Proc. IEEE Mil. Commun. Conf.*, Oct. 2018, pp. 1–6.
[7] F. Pancaldi, G. Vitetta, R. Kalbasi, N. Al-Dhahir, M. Uysal, and H. Mheidat, "Single-carrier frequency domain equalization," *IEEE Commun. Mag.*, vol. 25, no. 5, pp. 37–56, Sep. 2008.
[8] D. Jeong and J. Kim, "Signal detection for MIMO SC-FDMA systems exploiting block circulant channel structure," *IEEE Trans. Veh. Technol.*, vol. 65, no. 9, pp. 7774–7779, Sep. 2016.
[9] N. Benvenuto, R. Dinis, D. Falconer, and S. Tomasin, "Single carrier modulation with nonlinear frequency domain equalization: An idea whose time has come—again," *Proc. IEEE*, vol. 98, no. 1, pp. 69–96, Jan. 2010.
[10] X.-G. Xia, "Precoded and vector OFDM robust to channel spectral nulls and with reduced cyclic prefix length in single transmit antenna systems," *IEEE Trans. Commun.*, vol. 49, no. 8, pp. 1363–1374, Aug. 2001.
[11] Y. Li, I. Ngebani, X.-G. Xia, and A. Host-Madsen, "On performance of vector OFDM with linear receivers," *IEEE Trans. Signal Process.*, vol. 60, no. 10, pp. 5268–5280, Oct. 2012.
[12] J. Han, S. P. Chepuri, Q. Zhang, and G. Leus, "Iterative per-vector equalization for orthogonal signal-division multiplexing over time-varying underwater acoustic channels," *IEEE J. Ocean. Eng.*, vol. 44, no. 1, pp. 240–255, Jan. 2019.
[13] T. Ebihara and K. Mizutani, "Underwater acoustic communication with an orthogonal signal division multiplexing scheme in doubly spread channels," *IEEE J. Ocean. Eng.*, vol. 39, no. 1, pp. 47–58, Jan. 2014.
[14] T. Ebihara and G. Leus, "Doppler-resilient orthogonal signal-division multiplexing for underwater acoustic communication," *IEEE J. Ocean. Eng.*, vol. 41, no. 2, pp. 408–427, Apr. 2016.
[15] J. Han, L. Zhang, Q. Zhang, and G. Leus, "Low-complexity equalization of orthogonal signal-division multiplexing in doubly-selective channels," *IEEE Trans. Signal Process.*, vol. 67, no. 4, pp. 915–929, Feb. 2019.
[16] J. Han and G. Leus, "Space-time and space-frequency block coded vector OFDM modulation," *IEEE Commun. Lett.*, vol. 21, no. 1, pp. 204–207, Jan. 2017.
[17] T. Ebihara, G. Leus, and H. Ogasawara, "Underwater acoustic communication using multiple-input multiple-output Doppler-resilient orthogonal signal division multiplexing," in *Proc. OCEANS Conf.*, May 2018, pp. 1–4.